Challenges for molecular neuroimaging with MRI

Published in final edited form as:
Int J Imaging Syst Technol. 2010 March ; 20(1): 71–79. doi:10.1002/ima.20221.

Challenges for Molecular Neuroimaging with MRI

Victor S. Lelyveld, **Tatjana Atanasijevic**, and **Alan Jasanoff**
Department of Biological Engineering, Massachusetts Institute of Technology, NW14-2213, Cambridge, MA 02139

Abstract

Magnetic resonance (MRI)-based molecular imaging methods are beginning to have impact in neuroscience. A growing number of molecular imaging agents have been synthesized and tested in vitro, but so far relatively few have been validated in the brains of live animals. Here, we discuss key challenges associated with expanding the repertoire of successful molecular neuroimaging approaches. The difficulty of delivering agents past the blood-brain barrier (BBB) is a particular obstacle to molecular imaging in the central nervous system. We review established and emerging techniques for trans-BBB delivery, including intracranial infusion, BBB disruption, and transporter-related methods. Improving the sensitivity with which MRI-based molecular agents can be detected is a second major challenge. Better sensitivity would in turn reduce the requirements for delivery and alleviate potential side effects. We discuss recent efforts to enhance relaxivity of conventional longitudinal relaxation time (T_1) and transverse relaxation time (T_2) MRI contrast agents, as well as strategies that involve amplifying molecular signals or reducing endogenous background influences. With ongoing refinement of imaging approaches and brain delivery methods, MRI-based techniques for molecular-level neuroscientific investigation will fall increasingly within reach.

Keywords

MRI; brain; molecular; neuroimaging; contrast agent

I. INTRODUCTION

Molecular imaging agents have the potential to transform our understanding of brain physiology and function. Discovery of the hemoglobin-mediated blood oxygenation level dependent (BOLD) effect on magnetic resonance imaging (MRI) signal (Ogawa et al., 1990) and the mapping of radiolabeled tracer distribution using positron emission tomography (PET) (Phelps et al., 1975) have already had tremendous impact in both basic and clinical neuroscience. Despite these pioneering advances, it is not yet possible to use MRI- and PET-based approaches to answer arbitrary questions about molecular processes underlying brain function, largely because of limitations inherent in the physics of the imaging methods and probes themselves. Although PET methods can detect femtomolar levels of β-emitting compounds, resolution is usually limited to several millimeters, and studies of dynamic processes are only possible where significant redistribution of probes takes place. With MRI, a wide array of contrast mechanisms is available, and spatial and temporal resolution are typically more than an order of magnitude better than PET. On the other hand, the sensitivity

Correspondence to: Alan Jasanoff, Department of Biological Engineering, Massachusetts Institute of Technology, 150 Albany Street, NW14-2213, Cambridge, MA 02139; jasanoff@mit.edu.
Victor S. Lelyveld and Tatjana Atanasijevic have contributed equally to this work.

of MRI for existing molecular probes is relatively poor, and innovations in probe design and related in vivo methods are highly desirable.

Most molecular imaging agents for MRI have been developed over the past 10 years. Specific imaging agents have been created to target epitopes, track small molecules, measure changes in pH and ion concentrations, respond to enzymes, and report changes in gene expression. Most of the agents fall into four classes, based on the MRI contrast mechanisms they engage: (1) longitudinal relaxation time (T_1) agents, detected by T_1 relaxation-weighted MRI (Lauffer, 1987; Toth et al., 2001); (2) transverse relaxation time (T_2) agents, usually based on superparamagnetic iron oxide (SPIO), and detected by T_2 relaxation-weighted MRI (Muller et al., 2001); (3) chemical exchange saturation transfer (CEST) agents, monitored by a variant of magnetization transfer imaging (Sherry and Woods, 2008); and (4) heteronuclear agents, detected by nuclear magnetic resonance (NMR) signals from nuclei other than protons, most prominently ^{19}F (Yu et al., 2005a) or hyperpolarized ^{13}C (Mansson et al., 2006). Some agents convey information primarily as a function of their spatial distribution, whereas others sense or respond to targets in a manner affecting their NMR behavior (e.g., their relaxivity, the slope of $1/T_1$ or $1/T_2$ vs. probe concentration). Recent progress in MRI molecular imaging has been extensively reviewed (e.g., Allen and Meade, 2004; de Leon-Rodriguez et al., 2009; Sosnovik and Weissleder, 2007), and the potential for neuroscience applications has been recognized (Jasanoff, 2007; Meade et al., 2003). Despite the ingenuity invested in developing new agents, however, few are in wide-spread use for neuroimaging.

II. LESSONS FROM IN VIVO EXPERIMENTS

The difficulties associated with bringing MRI molecular neuroimaging into research practice are apparent when surveying the subset of the experimental strategies that have been validated so far in living brains. In most cases, large concentrations of contrast media are required, generally well over 10 μM. Further, the most successful strategies are those in which molecular imaging agents have been directed at relatively superficial analytes, or where the agents have been able to exploit endogenous mechanisms to reach their targets.

The most broadly applied molecular imaging method in neuroscience is based on injected paramagnetic Mn^{2+} ions that appear to accumulate in an activity-dependent manner in the brain by promiscuous uptake through neuronal voltage gated calcium channels (Lin and Koretsky, 1997; Pautler et al., 1998). Although Mn^{2+}-enhanced functional imaging was originally used in conjunction with blood-brain barrier (BBB) disruption (Lin and Koretsky, 1997; Aoki et al., 2002), subsequent applications have benefited from the fact that Mn^{2+} crosses the BBB, and can thus be injected directly into the bloodstream or peritoneum (Lee et al., 2005; Yu et al., 2005b). The ability to stimulate for long periods of time in the presence of Mn^{2+} has been critical to achieving reliable contrast, indicating that fairly high local concentrations of Mn^{2+} are necessary for detection (Silva et al., 2004). Like Mn^{2+}, and also in analogy to PET tracers, ^{13}C-labeled agents can exploit endogenous uptake mechanisms. Using hyperpolarization methods, the sensitivity with which ^{13}C compounds are detected can be boosted by many orders of magnitude (Ardenkjaer-Larsen et al., 2003), though their potential for some brain imaging applications may be hindered by limits on polarization lifetime. In recent in vivo applications, hyperpolarization-based imaging techniques have been applied to follow ^{13}C-labeled bicarbonate (Gallagher et al., 2008) and metabolites (Golman et al., 2006), each of which is associated with established families of transporters and processing enzymes.

Additional recent in vivo successes include agents designed to target relatively accessible physiological markers in the vasculature, and genetically encoded agents that avoid the need for exogenous delivery. Strong SPIO T_2 contrast agents have been designed to bind vascular

epitopes indicative of cerebral inflammation (van Kasteren et al., 2009; Serres et al., 2009). Upregulation of selectins on the vascular endothelium is detectable by the agents after intravenous injection (Sibson et al., 2004; Boutry et al., 2005). High iron concentrations were achieved by using relatively large particles (~80-nm diameter), and because cellular barriers and the BBB did not need to be traversed. Strategies for imaging vascular pH in the brain have also been feasible (Garcia-Martin et al., 2006), both because transport of pH sensors is not required after intravenous delivery, and because endogenous pH buffering is strong enough for the brain to tolerate large concentrations of contrast agents. Proof of principle experiments with genetically encoded contrast agents circumvented the delivery problem because the agents were biosynthesized endogenously (Gilad et al., 2008). To achieve adequate sensitivity, the genetic strategies introduced so far have also included a "multiplicative" aspect. Individual ferritin molecules (Genove et al., 2005; Cohen et al., 2007) each accumulate up to 2000 iron atoms per polypeptide 24-mer. MagA iron pumps (Zurkiya et al., 2008; Goldhawk et al., 2009) can presumably promote even larger iron to protein ratios. Individual protein CEST agents of moderate size (Gilad et al., 2007; McMahon et al., 2008) might reasonably provide on the order of 10^3 to 10^4 sites for labile proton exchange. All of these agents have for the most part been tested in contexts where high-level expression, perhaps in the order of 1 μM, is possible.

For the generic MRI molecular imaging agent, which may be highly polar, nanometer sized, or directed toward intracellular targets of exceptional significance, it is clearly not possible to rely on endogenous transport mechanisms for delivery into the brain or into cells. Although in some cases, it may be possible to engineer genetically encoded contrast agents to generate more complex functionality like responsiveness to intracellular signaling (Shapiro et al., 2009), genetically encoded species are generally less effective contrast agents than synthetic molecules, and of course could only be used in transgenic or transfected animals. For neuroimaging applications involving exogenous agents, efficient artificial delivery techniques are required. To mitigate difficulties associated with delivery, and to reduce potentially adverse effects of agents introduced into the brain, a closely related aim is required to improve MRI contrast agents, so that lower concentrations are required for detection. In the remainder of this review, we discuss critical challenges involved with developing effective strategies for molecular MRI in the brain, focusing particularly on advances in delivery methodology and sensitivity that may be critical to relatively near-term applications of newly developed molecular imaging agents in live animals.

III. STRATEGIES FOR DELIVERY OF MRI CONTRAST AGENTS TO THE BRAIN

Delivery of contrast agents designed for neuroimaging is particularly difficult because of the BBB, a specialized system of tight junctions between vascular endothelial cells and associated astrocytes that protects the brain from the potentially harmful substances in the bloodstream. The BBB restricts transport and diffusion of molecules between the brain and the cerebral vasculature. Only lipophilic molecules with molecular mass smaller than 400 Da are thought to cross the BBB passively by free diffusion (Pardridge, 2003). Some other types of molecules can transverse the BBB via endogenous active transport systems. The two most common transport processes across the BBB are carrier-mediated transport, for small water-soluble vitamins and nutrients; and receptor-mediated transport for certain large peptides and plasma proteins (Pardridge, 2005).

Because the BBB prevents brain delivery of diagnostic and therapeutic agents alike, techniques to bypass it have become the subject of extensive research. The best established trans-BBB delivery methods include invasive injection, as well as relatively noninvasive BBB disruption methods (Vykhodtseva et al., 2008). Intracerebral injection techniques are workhorse methods in neuroscience, both for delivery of imaging agents and for pharmacological treatments. Three

protocols are most commonly used: infusion through catheters implanted directly into brain tissue, intracerebroventricular infusion, and convection enhanced delivery (CED) using osmotic pumps or related devices (Pardridge, 2005). In addition to their invasiveness, the main limitation of these methods is the inhomogeneous and limited spread of molecules emanating from the delivery point. With sustained infusion, it is nevertheless possible to deliver agents to relatively large portions of a rodent brain. The approaches have been used to deliver MRI contrast agents to the brain, for example, the CED method has been employed recently to administer gadolinium diethylenetriamine pentaacetic acid (Gd-DTPA) (Mardor et al., 2005) and dextran-coated SPIO nanoparticles (Perlstein et al., 2008) to rat brains (Fig. 1A). These studies showed that relatively high-infusion rates (1–4 μM) achieved a volume of distribution corresponding to most of the striatum in injected animals.

Techniques for transient, reversible BBB disruption provide a mechanism for more homogeneous delivery of agents from the bloodstream into the brain parenchyma. BBB disruption has been linked to the onset of chronic neurological conditions in human subjects (Hawkins and Davis, 2005), but has not been shown to impair cognitive function on a time scale relevant to experimental studies in laboratory animals. The most traditional BBB disruption method is to administer a hyperosmotic shock to tight junctions in the cerebrovascular endothelium (Neuwelt and Rapoport, 1984). This can be performed by intravascular injection (typically through the carotid artery) of a hypertonic but otherwise inert solution such as 25% mannitol. Disruption following the shock persists for around an hour, during which substances can pass between the brain and bloodstream. Hyperosmotic shock methods are used clinically for treatment of conditions such as intracranial hypertension (Berger et al., 1995), ischemic stroke (Schwarz et al., 1998), and delivery of chemotherapeutic agents (Neuwelt et al., 1983); complications are noted only in a minority of cases (Elkassabany et al., 2008). In animals, hyperosmotic disruption of the BBB has been used to deliver Mn^{2+} in conjunction with neural activity-dependent labeling studies using MRI. Synthetic MRI contrast agents such as Gd-DTPA (Norman et al., 1991; Roman-Goldstein et al., 1994) and a variety of carbohydrate-coated SPIO nanoparticles (Muldoon et al., 2005) have been delivered to rodent brains after osmotic BBB disruption using mannitol (Fig. 1B). The most pronounced contrast changes were ipsilateral to the mannitol infusion, and were more homogeneous for the small molecule agent than for large nanoparticles.

A promising but more exploratory alternative to the hyperosmotic disruption technique uses focused ultrasound (FUS) to open the BBB (Vykhodtseva et al., 2008). Early studies of FUS-dependent BBB disruption found that ultrasonic energy deposition produced collateral damage to surrounding brain tissue (Bakay et al., 1956; Ballantine et al., 1960). It was later discovered that a sharp reduction in the FUS energy required for BBB opening is possible if gas-filled microbubbles (which act as ultrasound contrast agents) are injected into the bloodstream prior to sonication (Hynynen et al., 2001). Ultrasound-mediated BBB opening can be performed in MRI scanners and spatially targeted to discrete brain regions on a millimeter scale in rodents, making FUS considerably more versatile than hyperosmotic shock methods. Local BBB disruption with FUS seems to be possible without undesirable long-term effects (Hynynen et al., 2006). A wide variety of molecular species have been delivered to the brain using FUS methods, including Gd-DTPA and ~20-nm diameter SPIO contrast agents for MRI (Fig. 1C) (Hynynen et al., 2006; Liu et al., 2009), protein therapeutics (Kinoshita et al., 2006), and small molecules (Hynynen et al., 2005). Spatiotemporal characteristics of FUS-mediated BBB opening have not been completely characterized, but evidence suggests that the disruption persists for hours, and that larger blood vessels may be most susceptible to sonication (Choi et al., 2007).

The search for less disruptive strategies for trans-BBB delivery is an active area of research. Reported methods have employed carriers such as liposomes and nanoparticles (Huwyler et

al., 1996; Gulyaev et al., 1999). Additional efforts have focused on “molecular Trojan horse” strategies, in which a substrate for endogenous BBB transport systems is conjugated or fused to the molecule to be delivered, allowing it to be cotransported (Pardridge, 2008). Molecular Trojan horses include natural and engineered interaction partners targeted to the transferrin and insulin receptors, which have been examined in trial studies for their ability to promote transport of a number of therapeutic proteins and nucleic acids across the BBB (Pardridge, 2007). Nondisruptive trans-BBB delivery methods have been used in conjunction with a radiopharmaceutical for PET imaging (Lee et al., 2002) and with bacterial β-galactosidase, a reporter used for histological analysis (Zhang and Pardridge, 2005). Whether these methods can be effectively applied to deliver MRI contrast agents across the BBB is less certain, given the requirement in MRI for high-imaging agent concentrations.

A related Trojan horse approach has proved successful in the delivery of MRI contrast agents into cells through the plasma membrane (Dietz and Bahr, 2004). For imaging agents designed to sense intracellular targets in the brain, cell delivery is as critical a problem as transduction across the BBB. Both SPIO-based T_2 relaxation agents (Josephson et al., 1999) and small molecule T_1 contrast agents (Allen et al., 2004) have been reported to enter cells when conjugated to so-called cell penetrating peptides (CPPs), such as polyarginine and the tat peptide from human immunodeficiency virus (Zhao and Weissleder, 2004). CPP-mediated in vivo delivery of 70-nm fluorescent quantum dot nanoparticles to rat brain tissue (Santra et al., 2004) and cytosolic delivery of polyarginine-conjugated magnetic nanoparticles to implanted tumors in mice (Medarova et al., 2007) have been reported. DNA-facilitated delivery of magnetic nanoparticles in the mouse brain has also been described (Liu et al., 2007). An alternative strategy for cell delivery is to design imaging agents using paramagnetic complexes that are intrinsically membrane permeable. Paramagnetic metalloporphyrins have T_1 relaxivity comparable to traditional Gd^{3+}-polyaminocarboxylate complexes, and have been modified to form sensors internalized with high efficiency by cells (Zhang et al., 2007). Further development of agents with biochemical features explicitly conducive to brain or cellular delivery may be an important direction for future MRI molecular neuroimaging research.

IV. NEED FOR IMPROVED DETECTION OF MRI CONTRAST AGENTS

The preceding review of delivery strategies appropriate for MRI contrast agents shows that administration of exogenous agents to the brain is achievable, but not without potential complications. BBB opening techniques incur side effects, and less disruptive trans-BBB delivery methods are probably not yet efficient enough to carry MRI-detectable quantities of imaging agents into the brain. For all of the delivery techniques, there is a clear advantage to minimizing the amount of contrast agent required for imaging, and where large quantities of contrast agent are required, pathological side effects related to the agents themselves may also be incurred. Many MRI contrast agents incorporate paramagnetic heavy metals such as gadolinium and manganese, which as bare ions are extremely toxic even at low concentrations. Dissociated Gd^{3+}, for instance, inhibits calcium-dependent processes in cells (Cacheris et al., 1990), and induces a nephrotoxicity syndrome at doses of about 0.3 mmol/kg (Kuo et al., 2007). Chronic exposure to manganese is associated with neurological disorders (Olanow, 2004), hepatic failure (Chandra and Shukla, 1976), and cardiac toxicity (Wolf and Baum, 1983), and Mn^{2+} doses as low as 93 mg/kg for rats and 38 mg/kg for mice have been shown to cause serious adverse effects (Silva et al., 2004). SPIOs present a risk if iron escapes from nanoparticle cores (Longmire et al., 2008); chelation and additional treatments may be required in subjects where high doses of iron-containing contrast agents are used (Leite et al., 2002). Molecular functions performed by MRI contrast agents may also induce disruptions. For instance, an MRI probe designed to target a cell surface receptor will almost certainly interfere with receptor transport and binding of the molecule by its natural ligands. Perhaps less obviously, a responsive MRI contrast agent that binds protons, ions, or other analytes will

necessarily create buffering effects that disrupt normal physiology to an extent dependent on the concentration of the probe, as illustrated in Figure 2. Such complications are common to almost all drugs and imaging agents, but are especially severe for MRI molecular imaging probes, because of the high concentrations required. There is therefore a particularly acute need to improve the sensitivity of MRI detection of molecular imaging agents.

V. APPROACHES TO IMPROVING MOLECULAR IMAGING SENSITIVITY

T_1 agents based on chelated heavy metals are the MRI contrast agents most commonly used in the clinic, and have been the basis for molecular imaging agents with potential applications in the nervous system (Jasanoff, 2007). Clinically important complexes generally incorporate Gd^{3+} and exhibit T_1 relaxivities (r_1) in the 3–5 $mM^{-1}\ s^{-1}$ range at field strengths and temperatures typically used for research neuroimaging ($B_0 \geq 1.5$ T) (Laurent et al., 2006). In a biological sample with a background T_1 of 1 s, ~50 μM of an $r_1 = 4\ mM^{-1}\ s^{-1}$ complex would be required to produce a 20% signal change from background under strongly T_1-weighted imaging conditions (spin echo repetition time TR = 100 ms). As the relaxivity of the agent increases, the concentration required for a given level of signal change decreases proportionately. Prospects for increasing the relaxivity of static and responsive T_1 agents have been discussed in the literature (Werner et al., 2008; Aime et al., 2009; Caravan et al., 2009; de Leon-Rodriguez et al., 2009). Basic approaches have involved tuning the molecular parameters that determine r_1 and incorporating paramagnetic atoms into polymeric, macromolecular, or nanoscale frameworks. For instance, in an example shown in Figure 3A, a Gd-hydroxypyridonate (Gd-HOPO)-based complex was designed to have water exchange rate, rotational correlation time, and number of inner sphere water molecules optimized for high field (>20 MHz) relaxivity, while still maintaining stability against Gd^{3+} dissociation (Pierre et al., 2005). The novel Gd-HOPO agent had an r_1 of 18 $mM^{-1}\ s^{-1}$ (2.1 T, 25°C), roughly four times that of Gd-DTPA. The highest relaxivities reported at field strengths most commonly used for clinical imaging also include those of Gd-texaphyrin in 5% human serum albumin ($r_1 = 21\ mM^{-1}\ s^{-1}$, 1 T, 37°C) (Geraldes et al., 1995), a manganese analog of MS-325 in 660 μM rabbit serum albumin ($r_1 = 32\ mM^{-1}\ s^{-1}$, 1.4 T, 37°C) (Troughton et al., 2004), Gd-HOPO-based complexes conjugated to viral capsids ($r_1 = 31\ mM^{-1}\ s^{-1}$, 1.5 T, 25°C) (Datta et al., 2008), and Gd-decorated single-wall carbon nanotubes ($r_1 = 170\ mM^{-1}\ s^{-1}$, 1.5 T, 37°C) (Sitharaman and Wilson, 2006). Although some of the reported high-relaxivity agents may be too unstable or large for in vivo imaging, improvements in the area nevertheless suggest that r_1 values far in excess of current workhorse contrast agents might be approached at moderate field strengths (0.5–3 T). At field strengths now favored for small animal imaging (≥4.7 T), gains in r_1 are also possible, but likely to be less pronounced (Werner et al., 2008; Aime et al., 2009; Caravan et al., 2009; de Leon-Rodriguez et al., 2009).

The exceptionally large magnetic moments of superparamagnetic materials have inspired efforts to use SPIOs and related nanoparticles as cellular or molecular imaging agents both inside and outside the brain. Monocrystalline or polycrystalline iron oxide cores, ranging from 3 to 300 nm in diameter, can be passivated with hydrophilic surface chemistry to yield T_2 contrast agents with relaxivities (r_2) generally in the range from 50 to 200 $(mM\ Fe)^{-1}\ s^{-1}$ (Thorek et al., 2006; Sosnovik et al., 2008). In T_2-weighted imaging (spin echo time TE = 50 ms) with a background T_2 of 50 ms, an $r_2 = 150\ mM^{-1}\ s^{-1}$ SPIO colloid containing ~30 μM iron atoms (≪1 μM particles) would experience a 20% decrease in MRI signal from background. The fact that MRI signals are generally attenuated by SPIO agents has generally been considered to be a disadvantage, and has spawned a search for iron oxide-sensitive “positive contrast” techniques (Cunningham et al., 2005; Mani et al., 2006; Mills and Ahrens, 2009). Although SPIO contrast agents produce contrast changes more effectively than typical T_1 agents (particularly at high B_0), they must still be used at concentrations several order of magnitudes above those required for PET; for brain imaging, delivery and physiological

perturbations remain significant issues. Efforts to improve the relaxivity of SPIOs and other superparamagnetic agents are therefore also underway. High r_2 values have been measured with ferrite nanoparticles such as dimer-captosuccinic acid-solubilized $MnFe_2O_4$ and $CoFe_2O_4$ (r_2 = 228 and 393 mM^{-1} s^{-1}, respectively, at 9.4 T) (Lee et al., 2007; Kim et al., 2009). Tuning properties of the water-solubilizing surface chemistry applied to SPIOs can also boost their relaxivity; for instance, one study reported an extraordinary r_2 of 910 mM^{-1} s^{-1} (7 T, 25°C) for 10 nm SPIO cores coated in a polyacrylamide matrix (Moffat et al., 2003). In a further approach, micron-sized SPIOs with very high-total relaxivities have been used for MRI (Fig. 3B). These microparticles have been reported to allow individual cells to be visualized and tracked in the living brain (Shapiro et al., 2006).

Two alternatives to improving the relaxivity of conventional T_1 and T_2 MRI contrast agents are to use enzyme-based amplification strategies, and to employ imaging methods with reduced background signal. Enzymatic methods are exemplified by the demonstration approximately a decade ago that a T_1 agent sensitive to β-galactosidase, a commonly used reporter enzyme, could be constructed and used to map enzyme activity in whole frog embryos (Moats et al., 1997; Louie et al., 2000). Additional approaches have targeted contrast agents to myeloperoxidase (Bogdanov et al., 2002), tyrosinase (Weissleder et al., 1997), and matrix metalloproteases (Harris et al., 2006; Lepage et al., 2007). A related strategy noted earlier has been the use of metal transporters as genetic markers (Zurkiya et al., 2008; Goldhawk et al., 2009); amplification is produced because each protein can transport many paramagnetic metal ions.

As with imaging agents for other modalities, signal changes produced by MRI contrast agents may be difficult to detect either because they are small compared with scanner-related noise levels, or because of relatively high background from endogenous MRI signals, including physiological sources. The CEST technique provides one way to remove background influences, because the chemical shift of saturation can be varied to excite test or control proton pools (Sherry and Woods, 2008). The chemical-shift dependence of CEST has allowed pH mapping and reporter gene detection in the brain, and facilitates creation of “ratiometric” CEST molecular imaging probes (Ward et al., 2000), where analyte measurement does not depend on the concentration of the probe, as well as “multicolor” agents that can be imaged in parallel because they have different saturation frequencies (McMahon et al., 2008). Although CEST contrast usually relies on long saturation times and millimolar concentrations of protons with chemical shifts resolved from water, it has been suggested that CEST agents that incorporate paramagnetic lanthanides could be detected at submicromolar levels (Zhang et al., 2003); improved sensitivity might also be achieved using superparamagnetic nanostructures as CEST-like agents (Zabow et al., 2008). Heteronuclear imaging agents provide an alternative way to improve molecular imaging performance by minimizing background. ^{19}F is the most common isotope of fluorine and can be detected relatively efficiently by MRI, but is not present endogenously in the body. Both unresponsive and responsive ^{19}F probes have been synthesized (Yu et al., 2005a), and ^{19}F imaging agents have been used recently in the brain in contexts where large local ^{19}F levels were obtainable and relatively low resolutions were used for scanning (Higuchi et al., 2005; Porcari et al., 2008; Ruiz-Cabello et al., 2008). In some cases, it is possible to synthesize fluorinated analogs of previously characterized compounds to produce MRI-detectable tracers with properties similar to the parent molecules; this approach was used in a recent demonstration of amyloid plaque detection by ^{19}F MRI (Fig. 3C) (Higuchi et al., 2005). Hyperpolarized ^{13}C agents can be constructed in similar fashion and may be imaged with no noticeable contribution from endogenous ^{13}C (Ardenkjaer-Larsen et al., 2003), but currently only over periods on the order of a minute. Extending the utility of hyperpolarization-based molecular imaging may require nuclei with longer lasting polarization lifetimes (long T_1) (Dementyev et al., 2008), or continuous polarization methods (Brunner et al., 1999; McCarney et al., 2007). A sensitive technique for molecular imaging based on

hyperpolarized ^{129}Xe gas and targeted Xe-binding cryptophane cages has also been proposed (Hilty et al., 2005; Schröder et al., 2006), and may have interesting advantages.

VI. CONCLUSION

The unique capabilities of MRI for studying molecular processes in vivo were recognized early in the history of the technique, as was the potential utility of MRI contrast agents (Lauterbur, 1980). In the intervening decades, a noteworthy effort has gone into design of imaging agents and approaches for detecting molecular targets in the nervous system. A number of MRI molecular neuroimaging approaches have now been reported to have met the requirements for brain delivery and sensitivity well enough to be validated in vivo. Recent improvements in MRI imaging agents and the methods required for them to access targets in the brain suggest that the list could be considerably expanded in the future. Although significant challenges remain, an MRI-based toolbox for relatively noninvasive molecular neuroimaging at the whole-brain level in animals could be within reach of today's technology.

Acknowledgments

Grant Sponsors: Raymond and Beverley Sackler Foundation, NIH (R01-DA28299, DP2-OD2441)

REFERENCES

Aime S, Botta M, Crich SG, Giovenzana G, Pagliarin R, Sisti M, Terreno E. NMR relaxometric studies of Gd(III) complexes with heptadentate macrocyclic ligands. Magn Reson Chem 1998;36:S200–S208.

Aime S, Castelli DD, Crich SG, Gianolio E, Terreno E. Pushing the sensitivity envelope of lanthanide-based magnetic resonance imaging (MRI) contrast agents for molecular imaging applications. Acc Chem Res 2009;42:822–831. [PubMed: 19534516]

Allen MJ, MacRenaris KW, Venkatasubramanian PN, Meade TJ. Cellular delivery of MRI contrast agents. Chem Biol 2004;11:301–307. [PubMed: 15123259]

Allen MJ, Meade TJ. Magnetic resonance contrast agents for medical and molecular imaging. Met Ions Biol Syst 2004;42:1–38. [PubMed: 15206098]

Aoki I, Tanaka C, Takegami T, Ebisu T, Umeda M, Fukunaga M, Fukuda K, Silva AC, Koretsky AP, Naruse S. Dynamic activity-induced manganese-dependent contrast magnetic resonance imaging (DAIM MRI). Magn Reson Med 2002;48:927–933. [PubMed: 12465100]

Ardenkjaer-Larsen JH, Fridlund B, Gram A, Hansson G, Hansson L, Lerche MH, Servin R, Thaning M, Golman K. Increase in signal-to-noise ratio of >10,000 times in liquid-state NMR. Proc Natl Acad Sci USA 2003;100:10158–10163. [PubMed: 12930897]

Bakay L, Ballantine HT Jr, Hueter TF, Sosa D. Ultrasonically produced changes in the blood-brain barrier. AMA Arch Neurol Psychiatry 1956;76:457–467.

Ballantine HT Jr, Bell E, Manlapaz J. Progress and problems in the neurological applications of focused ultrasound. J Neurosurg 1960;17:858–876. [PubMed: 13686380]

Berger S, Schurer L, Hartl R, Messmer K, Baethmann A. Reduction of post-traumatic intracranial hypertension by hypertonic/hyperoncotic saline/dextran and hypertonic mannitol. Neurosurgery 1995;37:98–107. discussion 107–108. [PubMed: 8587698]

Bogdanov A Jr, Matuszewski L, Bremer C, Petrovsky A, Weissleder R. Oligomerization of paramagnetic substrates result in signal amplification and can be used for MR imaging of molecular targets. Mol Imaging 2002;1:16–23. [PubMed: 12920857]

Boutry S, Burtea C, Laurent S, Toubeau G, Vander Elst L, Muller RN. Magnetic resonance imaging of inflammation with a specific selectin-targeted contrast agent. Magn Reson Med 2005;53:800–807. [PubMed: 15799062]

Brunner E, Haake M, Kaiser L, Pines A, Reimer JA. Gas flow MRI using circulating laser-polarized 129Xe. J Magn Reson 1999;138:155–159. [PubMed: 10329238]

Cacheris WP, Quay SC, Rocklage SM. The relationship between thermodynamics and the toxicity of gadolinium complexes. Magn Reson Imaging 1990;8:467–481. [PubMed: 2118207]

Caravan P, Ellison JJ, McMurry TJ, Lauffer RB. Gadolinium(III) chelates as MRI contrast agents: Structure, dynamics, and applications. Chem Rev 1999;99:2293–2352. [PubMed: 11749483]

Caravan P, Farrar CT, Frullano L, Uppal R. Influence of molecular parameters and increasing magnetic field strength on relaxivity of gadolinium- and manganese-based T1 contrast agents. Contrast Media Mol Imaging 2009;4:89–100. [PubMed: 19177472]

Chandra SV, Shukla GS. Role of iron deficiency in inducing susceptibility to manganese toxicity. Arch Toxicol 1976;35:319–323. [PubMed: 989299]

Choi JJ, Pernot M, Brown TR, Small SA, Konofagou EE. Spatiotemporal analysis of molecular delivery through the blood-brain barrier using focused ultrasound. Phys Med Biol 2007;52:5509–5530. [PubMed: 17804879]

Cohen B, Ziv K, Plaks V, Israely T. MRI detection of transcriptional regulation of gene expression in transgenic mice. Nat Med 2007;13:498–503. [PubMed: 17351627]

Cohen SM, Xu J, Radkov E, Raymond KN, Botta M, Barge A, Aime S. Syntheses and relaxation properties of mixed gadolinium hydroxypyridinonate MRI contrast agents. Inorg Chem 2000;39:5747–5756. [PubMed: 11151375]

Cunningham CH, Arai T, Yang PC, McConnell MV, Pauly JM, Conolly SM. Positive contrast magnetic resonance imaging of cells labeled with magnetic nanoparticles. Magn Reson Med 2005;53:999–1005. [PubMed: 15844142]

Datta A, Hooker JM, Botta M, Francis MB, Aime S, Raymond KN. High relaxivity gadolinium hydroxypyridonate-viral capsid conjugates: Nanosized MRI contrast agents. J Am Chem Soc 2008;130:2546–2552. [PubMed: 18247608]

de Leon-Rodriguez LM, Lubag AJ, Malloy CR, Martinez GV, Gillies RJ, Sherry AD. Responsive MRI agents for sensing metabolism in vivo. Acc Chem Res 2009;42:948–957. [PubMed: 19265438]

Dementyev AE, Cory DG, Ramanathan C. Dynamic nuclear polarization in silicon microparticles. Phys Rev Lett 2008;100:127601. [PubMed: 18517909]

Dietz GP, Bahr M. Delivery of bioactive molecules into the cell: The Trojan horse approach. Mol Cell Neurosci 2004;27:85–131. [PubMed: 15485768]

Elkassabany NM, Bhatia J, Deogaonkar A, Barnett GH, Lotto M, Maurtua M, Ebrahim Z, Schubert A, Ference S, Farag E. Perioperative complications of blood brain barrier disruption under general anesthesia: A retrospective review. J Neurosurg Anesthesiol 2008;20:45–48. [PubMed: 18157025]

Gallagher FA, Kettunen MI, Day SE, Hu DE, Ardenkjaer-Larsen JH, Zandt R, Jensen PR, Karlsson M, Golman K, Lerche MH, Brindle KM. Magnetic resonance imaging of pH in vivo using hyperpolarized 13C-labelled bicarbonate. Nature 2008;453:940–943. [PubMed: 18509335]

Garcia-Martin ML, Martinez GV, Raghunand N, Sherry AD, Zhang S, Gillies RJ. High resolution pH(e) imaging of rat glioma using pH-dependent relaxivity. Magn Reson Med 2006;55:309–315. [PubMed: 16402385]

Genove G, DeMarko U, Xu H, Goins WF, Ahrens ET. A new transgene reporter for in vivo magnetic resonance imaging. Nat Med 2005;11:450–454. [PubMed: 15778721]

Geraldes CF, Sherry AD, Vallet P, Maton F, Muller RN, Mody TD, Hemmi G, Sessler JL. Nuclear magnetic relaxation dispersion studies of water-soluble gadolinium(III)-texaphyrin complexes. J Magn Reson Imaging 1995;5:725–729. [PubMed: 8748493]

Gilad AA, McMahon MT, Walczak P, Winnard PT Jr, Raman V, van Laarhoven HW, Skoglund CM, Bulte JW, van Zijl PC. Artificial reporter gene providing MRI contrast based on proton exchange. Nat Biotechnol 2007;25:217–219. [PubMed: 17259977]

Gilad AA, Ziv K, McMahon MT, van Zijl PC, Neeman M, Bulte JW. MRI reporter genes. J Nucl Med 2008;49:1905–1908. [PubMed: 18997049]

Goldhawk DE, Lemaire C, McCreary CR, McGirr R, Dhanvantari S, Thompson RT, Figueredo R, Koropatnick J, Foster P, Prato FS. Magnetic resonance imaging of cells overexpressing MagA, an endogenous contrast agent for live cell imaging. Mol Imaging 2009;8:129–139. [PubMed: 19723470]

Golman K, In't Zandt R, Thaning M. Real-time metabolic imaging. Proc Natl Acad Sci USA 2006;103:11270–11275. [PubMed: 16837573]

Gulyaev AE, Gelperina SE, Skidan IN, Antropov AS, Kivman GY, Kreuter J. Significant transport of doxorubicin into the brain with polysorbate 80-coated nanoparticles. Pharm Res 1999;16:1564–1569. [PubMed: 10554098]

Harris TJ, von Maltzahn G, Derfus AM, Ruoslahti E, Bhatia SN. Proteolytic actuation of nanoparticle self-assembly. Angew Chem Int Ed Engl 2006;45:3161–3165. [PubMed: 16642514]

Hawkins BT, Davis TP. The blood-brain barrier/neurovascular unit in health and disease. Pharmacol Rev 2005;57:173–185. [PubMed: 15914466]

Helmchen, F.; Tank, D. “A single-compartment model of calcium dynamics in nerve terminals and dendrites,”. In: Yuste, R.; Konnerth, A., editors. Imaging in neuroscience and development: A laboratory manual. Cold Spring Harbor, NY: Cold Spring Harbor Laboratory Press; 2005. p. 265-275.

Higuchi M, Iwata N, Matsuba Y, Sato K, Sasamoto K, Saido TC. 19F and 1H MRI detection of amyloid beta plaques in vivo. Nat Neurosci 2005;8:527–533. [PubMed: 15768036]

Hilty C, Lowery TJ, Wemmer DE, Pines A. Spectrally resolved magnetic resonance imaging of a xenon biosensor. Angew Chem Int Ed Engl 2005;45:70–73. [PubMed: 16311999]

Huwyler J, Wu D, Pardridge WM. Brain drug delivery of small molecules using immunoliposomes. Proc Natl Acad Sci USA 1996;93:14164–14169. [PubMed: 8943078]

Hynynen K, McDannold N, Sheikov NA, Jolesz FA, Vykhodtseva N. Local and reversible blood-brain barrier disruption by noninvasive focused ultrasound at frequencies suitable for trans-skull sonications. Neuroimage 2005;24:12–20. [PubMed: 15588592]

Hynynen K, McDannold N, Vykhodtseva N, Jolesz FA. Noninvasive MR imaging-guided focal opening of the blood-brain barrier in rabbits. Radiology 2001;220:640–646. [PubMed: 11526261]

Hynynen K, McDannold N, Vykhodtseva N, Raymond S, Weissleder R, Jolesz FA, Sheikov N. Focal disruption of the blood-brain barrier due to 260-kHz ultrasound bursts: A method for molecular imaging and targeted drug delivery. J Neurosurg 2006;105:445–454. [PubMed: 16961141]

Jasanoff A. MRI contrast agents for functional molecular imaging of brain activity. Curr Opin Neurobiol 2007;17:593–600. [PubMed: 18093824]

Josephson L, Tung CH, Moore A, Weissleder R. High-efficiency intracellular magnetic labeling with novel superparamagnetic-Tat peptide conjugates. Bioconjug Chem 1999;10:186–191. [PubMed: 10077466]

Kim D-H, Zeng H, Ng TC, Brazel CS. T1 and T2 relaxivities of succimer-coated MF23+O4 (M = Mn^{2+}, Fe^{2+} and Co^{2+}) inverse spinel ferrites for potential use as phase-contrast agents in medical MRI. J Magn Magn Mater 2009;321:3899–3904.

Kinoshita M, McDannold N, Jolesz FA, Hynynen K. Noninvasive localized delivery of Herceptin to the mouse brain by MRI-guided focused ultrasound-induced blood-brain barrier disruption. Proc Natl Acad Sci USA 2006;103:11719–11723. [PubMed: 16868082]

Kroll RA, Pagel MA, Muldoon LL, Roman-Goldstein S, Fiamengo SA, Neuwelt EA. Improving drug delivery to intracerebral tumor and surrounding brain in a rodent model: A comparison of osmotic versus bradykinin modification of the blood-brain and/or blood-tumor barriers. Neurosurgery 1998;43:879–886. discussion 886–879. [PubMed: 9766316]

Kuo PH, Kanal E, Abu-Alfa AK, Cowper SE. Gadolinium-based MR contrast agents and nephrogenic systemic fibrosis. Radiology 2007;242:647–649. [PubMed: 17213364]

Lauffer RE. Paramagnetic metal complexes as water proton relaxation agents for NMR imaging: Theory and design. Chem Rev 1987;87:901–927.

Laurent S, Elst LV, Muller RN. Comparative study of the physicochemical properties of six clinical low molecular weight gadolinium contrast agents. Contrast Media Mol Imaging 2006;1:128–137. [PubMed: 17193689]

Lauterbur PC. Progress in n.m.r. zeugmatography imaging. Philos Trans R Soc Lond B Biol Sci 1980;289:483–487. [PubMed: 6106222]

Lee HJ, Zhang Y, Zhu C, Duff K, Pardridge WM. Imaging brain amyloid of Alzheimer disease in vivo in transgenic mice with an Abeta peptide radiopharmaceutical. J Cereb Blood Flow Metab 2002;22:223–231. [PubMed: 11823720]

Lee J-H, Huh Y-M, Jun Y-W, Seo J-W, Jang J-T, Song H-T, Kim S, Cho E-J, Yoon H-G, Suh J-S, Cheon J. Artificially engineered magnetic nanoparticles for ultra-sensitive molecular imaging. Nat Med 2007;13:95–99. [PubMed: 17187073]

Lee JH, Silva AC, Merkle H, Koretsky AP. Manganese-enhanced magnetic resonance imaging of mouse brain after systemic administration of $MnCl_2$: Dose-dependent and temporal evolution of T1 contrast. Magn Reson Med 2005;53:640–648. [PubMed: 15723400]

Leite FP, Tsao D, Vanduffel W, Fize D, Sasaki Y, Wald LL, Dale AM, Kwong KK, Orban GA, Rosen BR, Tootell RB, Mandeville JB. Repeated fMRI using iron oxide contrast agent in awake, behaving macaques at 3 Tesla. Neuroimage 2002;16:283–294. [PubMed: 12030817]

Lepage M, Dow WC, Melchior M, You Y, Fingleton B, Quarles CC, Pepin C, Gore JC, Matrisian LM, McIntyre JO. Noninvasive detection of matrix metalloproteinase activity in vivo using a novel magnetic resonance imaging contrast agent with a solubility switch. Mol Imaging 2007;6:393–403. [PubMed: 18053410]

Lin YJ, Koretsky AP. Manganese ion enhances T1-weighted MRI during brain activation: An approach to direct imaging of brain function. Magn Reson Med 1997;38:378–388. [PubMed: 9339438]

Liu CH, Kim YR, Ren JQ, Eichler F, Rosen BR, Liu PK. Imaging cerebral gene transcripts in live animals. J Neurosci 2007;27:713–722. [PubMed: 17234603]

Liu HL, Hsu PH, Chu PC, Wai YY, Chen JC, Shen CR, Yen TC, Wang JJ. Magnetic resonance imaging enhanced by superparamagnetic iron oxide particles: Usefulness for distinguishing between focused ultrasound-induced blood-brain barrier disruption and brain hemorrhage. J Magn Reson Imaging 2009;29:31–38. [PubMed: 19097103]

Longmire M, Choyke PL, Kobayashi H. Clearance properties of nano-sized particles and molecules as imaging agents: Considerations and caveats. Nanomed 2008;3:703–717.

Louie AY, Hüber MM, Ahrens ET, Rothbächer U, Moats R, Jacobs RE, Fraser SE, Meade TJ. In vivo visualization of gene expression using magnetic resonance imaging. Nat Biotechnol 2000;18:321–325. [PubMed: 10700150]

Mani V, Briley-Saebo KC, Itskovich VV, Samber DD, Fayad ZA. Gradient echo acquisition for superparamagnetic particles with positive contrast (GRASP): Sequence characterization in membrane and glass superparamagnetic iron oxide phantoms at 1.5T and 3T. Magn Reson Med 2006;55:126–135. [PubMed: 16342148]

Mansson S, Johansson E, Magnusson P, Chai CM, Hansson G, Petersson JS, Stahlberg F, Golman K. 13C imaging-a new diagnostic platform. Eur Radiol 2006;16:57–67. [PubMed: 16402256]

Mardor Y, Rahav O, Zauberman Y, Lidar Z, Ocherashvilli A, Daniels D, Roth Y, Maier SE, Orenstein A, Ram Z. Convection-enhanced drug delivery: Increased efficacy and magnetic resonance image monitoring. Cancer Res 2005;65:6858–6863. [PubMed: 16061669]

McCarney ER, Armstrong BD, Lingwood MD, Han S. Hyperpolarized water as an authentic magnetic resonance imaging contrast agent. Proc Natl Acad Sci USA 2007;104:1754–1759. [PubMed: 17264210]

McMahon MT, Gilad AA, DeLiso MA, Berman SM, Bulte JW, van Zijl PC. New “multicolor” polypeptide diamagnetic chemical exchange saturation transfer (DIACEST) contrast agents for MRI. Magn Reson Med 2008;60:803–812. [PubMed: 18816830]

Meade TJ, Taylor AK, Bull SR. New magnetic resonance contrast agents as biochemical reporters. Curr Opin Neurobiol 2003;13:597–602. [PubMed: 14630224]

Medarova Z, Pham W, Farrar C, Petkova V, Moore A. In vivo imaging of siRNA delivery and silencing in tumors. Nat Med 2007;13:372–377. [PubMed: 17322898]

Mills PH, Ahrens ET. Enhanced positive-contrast visualization of paramagnetic contrast agents using phase images. Magn Reson Med 2009;62:1349–1355. [PubMed: 19780169]

Moats RA, Fraser SE, Meade TJ. “smart“ magnetic resonance imaging agent that reports on specific enzyme activity. Angew Chem Int Ed Engl 1997;36:726–728.

Moffat BA, Reddy GR, McConville P, Hall DE, Chenevert TL, Kopelman RR, Philbert M, Weissleder R, Rehemtulla A, Ross BD. A novel polyacrylamide magnetic nanoparticle contrast agent for molecular imaging using MRI. Mol Imaging 2003;2:324–332. [PubMed: 14717331]

Muldoon LL, Sandor M, Pinkston KE, Neuwelt EA. Imaging, distribution, and toxicity of superparamagnetic iron oxide magnetic resonance nanoparticles in the rat brain and intracerebral tumor. Neurosurgery 2005;57:785–796. discussion 785–796. [PubMed: 16239893]

Muller, RN.; Roch, A.; Colet, J-M.; Ouakssim, A.; Gillis, P. Particulate magnetic contrast agents. In: Merbach, AE.; Toth, E., editors. The chemistry of contrast agents in medical magnetic resonance imaging. New York: Wiley; 2001.

Neuwelt EA, Balaban E, Diehl J, Hill S, Frenkel E. Successful treatment of primary central nervous system lymphomas with chemotherapy after osmotic blood-brain barrier opening. Neurosurgery 1983;12:662–671. [PubMed: 6410302]

Neuwelt EA, Rapoport SI. Modification of the blood-brain barrier in the chemotherapy of malignant brain tumors. Fed Proc 1984;43:214–219. [PubMed: 6692941]

Norman AB, Bertram KJ, Thomas SR, Pratt RG, Samaratunga RC, Sanberg PR. Magnetic resonance imaging of rat brain following in vivo disruption of the cerebral vasculature. Brain Res Bull 1991;26:593–597. [PubMed: 1907878]

Ogawa S, Lee T, Kay A, Tank D. Brain magnetic resonance imaging with contrast dependent on blood oxygenation. Proc Natl Acad Sci USA 1990;87:9868–9872. [PubMed: 2124706]

Olanow CW. Manganese-induced parkinsonism and Parkinson's disease. Ann NY Acad Sci 2004;1012:209–223. [PubMed: 15105268]

Pardridge WM. Blood-brain barrier drug targeting: The future of brain drug development. Mol Interv 2003;3:90–105. 151. [PubMed: 14993430]

Pardridge WM. The blood-brain barrier: Bottleneck in brain drug development. NeuroRx 2005;2:3–14. [PubMed: 15717053]

Pardridge WM. Drug targeting to the brain. Pharm Res 2007;24:1733–1744. [PubMed: 17554607]

Pardridge WM. Re-engineering biopharmaceuticals for delivery to brain with molecular Trojan horses. Bioconjug Chem 2008;19:1327–1338. [PubMed: 18547095]

Pautler RG, Silva AC, Koretsky AP. In vivo neuronal tract tracing using manganese-enhanced magnetic resonance imaging. Magn Reson Med 1998;40:740–748. [PubMed: 9797158]

Perlstein B, Ram Z, Daniels D, Ocherashvilli A, Roth Y, Margel S, Mardor Y. Convection-enhanced delivery of maghemite nanoparticles: Increased efficacy and MRI monitoring. Neuro Oncol 2008;10:153–161. [PubMed: 18316474]

Phelps M, Hoffmann E, Mullani N, Ter-Pogossian M. Application of annihilation coincidence detection to transaxial reconstruction tomography. J Nucl Med 1975;16:210–224. [PubMed: 1113170]

Pierre VC, Botta M, Raymond KN. Dendrimeric gadolinium chelate with fast water exchange and high relaxivity at high magnetic field strength. J Am Chem Soc 2005;127:504–505. [PubMed: 15643857]

Porcari P, Capuani S, D'Amore E, Lecce M, La Bella A, Fasano F, Campanella R, Migneco LM, Pastore FS, Maraviglia B. In vivo (19)F MRI and (19)F MRS of (19)F-labelled boronophenylalanine-fructose complex on a C6 rat glioma model to optimize boron neutron capture therapy (BNCT). Phys Med Biol 2008;53:6979–6989. [PubMed: 19001698]

Roman-Goldstein SM, Barnett PA, McCormick CI, Szumowski J, Shannon EM, Ramsey FL, Mass M, Neuwelt EA. Effects of Gd-DTPA after osmotic BBB disruption in a rodent model: Toxicity and MR findings. J Comput Assist Tomogr 1994;18:731–736. [PubMed: 8089321]

Ruiz-Cabello J, Walczak P, Kedziorek DA, Chacko VP, Schmieder AH, Wickline SA, Lanza GM, Bulte JW. In vivo "hot spot" MR imaging of neural stem cells using fluorinated nanoparticles. Magn Reson Med 2008;60:1506–1511. [PubMed: 19025893]

Santra S, Yang H, Dutta D, Stanley JT, Holloway PH, Tan W, Moudgil BM, Mericle RA. TAT conjugated, FITC doped silica nanoparticles for bioimaging applications. Chem Commun (Camb) 2004:2810–2811. [PubMed: 15599418]

Schröder L, Lowery TJ, Hilty C, Wemmer DE, Pines A. Molecular imaging using a targeted magnetic resonance hyperpolarized biosensor. Science (New York, NY) 2006;314:446–449.

Schwarz S, Schwab S, Bertram M, Aschoff A, Hacke W. Effects of hypertonic saline hydroxyethyl starch solution and mannitol in patients with increased intracranial pressure after stroke. Stroke 1998;29:1550–1555. [PubMed: 9707191]

Serres S, Anthony DC, Jiang Y, Broom KA, Campbell SJ, Tyler DJ, van Kasteren SI, Davis BG, Sibson NR. Systemic inflammatory response reactivates immune-mediated lesions in rat brain. J Neurosci 2009;29:4820–4828. [PubMed: 19369550]

Shapiro EM, Sharer K, Skrtic S, Koretsky AP. In vivo detection of single cells by MRI. Magn Reson Med 2006;55:242–249. [PubMed: 16416426]

Shapiro M, Szablowski J, Langer R, Jasanoff A. Protein nanoparticles engineered to sense kinase activity in MRI. J Am Chem Soc 2009;131:2484–2486. [PubMed: 19199639]

Sherry AD, Woods M. Chemical exchange saturation transfer contrast agents for magnetic resonance imaging. Annu Rev Biomed Eng 2008;10:391–411. [PubMed: 18647117]

Sibson NR, Blamire AM, Bernades-Silva M, Laurent S, Boutry S, Muller RN, Styles P, Anthony DC. MRI detection of early endothelial activation in brain inflammation. Magn Reson Med 2004;51:248–252. [PubMed: 14755648]

Silva AC, Lee JH, Aoki I, Koretsky AP. Manganese-enhanced magnetic resonance imaging (MEMRI): Methodological and practical considerations. NMR Biomed 2004;17:532–543. [PubMed: 15617052]

Sitharaman B, Wilson LJ. Gadonanotubes as new high-performance MRI contrast agents. Int J Nanomedicine 2006;1:291–295. [PubMed: 17717970]

Skovronsky DM, Zhang B, Kung MP, Kung HF, Trojanowski JQ, Lee VM. In vivo detection of amyloid plaques in a mouse model of Alzheimer's disease. Proc Natl Acad Sci USA 2000;97:7609–7614. [PubMed: 10861023]

Sosnovik DE, Nahrendorf M, Weissleder R. Magnetic nanoparticles for MR imaging: Agents, techniques and cardiovascular applications. Basic Res Cardiol 2008;103:122–130. [PubMed: 18324368]

Sosnovik DE, Weissleder R. Emerging concepts in molecular MRI. Curr Opin Biotechnol 2007;18:4–10. [PubMed: 17126545]

Thorek DLJ, Chen AK, Czupryna J, Tsourkas A. Superparamagnetic iron oxide nanoparticle probes for molecular imaging. Ann Biomed Eng 2006;34:23–38. [PubMed: 16496086]

Toth, E.; Helm, L.; Merbach, AE. Relaxivity of gadolinium(III) complexes: Theory and mechanism. In: Merbach, AE.; Toth, E., editors. The chemistry of contrast agents in medical magnetic resonance imaging. New York: Wiley; 2001.

Treat LH, McDannold N, Vykhodtseva N, Zhang Y, Tam K, Hynynen K. Targeted delivery of doxorubicin to the rat brain at therapeutic levels using MRI-guided focused ultrasound. Int J Cancer 2007;121:901–907. [PubMed: 17437269]

Troughton JS, Greenfield MT, Greenwood JM, Dumas S, Wiethoff AJ, Wang J, Spiller M, McMurry TJ, Caravan P. Synthesis and evaluation of a high relaxivity manganese(II)-based MRI contrast agent. Inorg Chem 2004;43:6313–6323. [PubMed: 15446878]

van Kasteren SI, Campbell SJ, Serres S, Anthony DC, Sibson NR, Davis BG. Glyconanoparticles allow pre-symptomatic in vivo imaging of brain disease. Proc Natl Acad Sci USA 2009;106:18–23. [PubMed: 19106304]

Vykhodtseva N, McDannold N, Hynynen K. Progress and problems in the application of focused ultrasound for blood-brain barrier disruption. Ultrasonics 2008;48:279–296. [PubMed: 18511095]

Ward KM, Aletras AH, Balaban RS. A new class of contrast agents for MRI based on proton chemical exchange dependent saturation transfer (CEST). J Magn Reson 2000;143:79–87. [PubMed: 10698648]

Weissleder R, Simonova M, Bogdanova A, Bredow S, Enochs WS, Bogdanov A Jr. MR imaging and scintigraphy of gene expression through melanin induction. Radiology 1997;204:425–429. [PubMed: 9240530]

Werner EJ, Datta A, Jocher CJ, Raymond KN. High-relaxivity MRI contrast agents: Where coordination chemistry meets medical imaging. Angew Chem Int Ed Engl 2008;47:8568–8580. [PubMed: 18825758]

Wolf GL, Baum L. Cardiovascular toxicity and tissue proton T1 response to manganese injection in the dog and rabbit. AJR Am J Roentgenol 1983;141:193–197. [PubMed: 6305179]

Yu JX, Kodibagkar VD, Cui W, Mason RP. 19F: A versatile reporter for non-invasive physiology and pharmacology using magnetic resonance. Curr Med Chem 2005a;12:819–848. [PubMed: 15853714]

Yu X, Wadghiri YZ, Sanes DH, Turnbull DH. In vivo auditory brain mapping in mice with Mn-enhanced MRI. Nat Neurosci 2005b;8:961–968. [PubMed: 15924136]

Zabow G, Dodd S, Moreland J, Koretsky A. Micro-engineered local field control for high-sensitivity multispectral MRI. Nature 2008;453:1058–1063. [PubMed: 18563157]

Zhang S, Merritt M, Woessner DE, Lenkinski RE, Sherry AD. PARACEST agents: Modulating MRI contrast via water proton exchange. Acc Chem Res 2003;36:783–790. [PubMed: 14567712]

Zhang X-A, Lovejoy KS, Jasanoff A, Lippard SJ. Water-soluble porphyrins as a dual-function molecular imaging platform for MRI and fluorescence zinc sensing. Proc Natl Acad Sci USA 2007;104:10780–10785. [PubMed: 17578918]

Zhang Y, Pardridge WM. Delivery of beta-galactosidase to mouse brain via the blood-brain barrier transferrin receptor. J Pharmacol Exp Ther 2005;313:1075–1081. [PubMed: 15718287]

Zhao M, Weissleder R. Intracellular cargo delivery using tat peptide and derivatives. Med Res Rev 2004;24:1–12. [PubMed: 14595670]

Zurkiya O, Chan AW, Hu X. MagA is sufficient for producing magnetic nanoparticles in mammalian cells, making it an MRI reporter. Magn Reson Med 2008;59:1225–1231. [PubMed: 18506784]

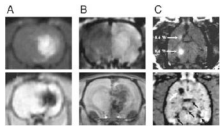

Figure 1.

Delivery of T_1 and T_2 contrast agents to the brain. A: Coronal MRI scans obtained after convection enhanced delivery of 1:70 Gd-DTPA [top; Mardor et al. (2005)] or 0.2 mg/mL dextran-coated ~80-nm diameter SPIOs [bottom; Perlstein et al. (2008)] to rat brain. Infusion rates were 1–4 μL/min over 15–90 min periods. B: Delivery of gadolinium-based [top; Kroll et al. (1998)] and iron oxide [bottom; Muldoon et al. (2005)] contrast agents to rat brain following 25% mannitol-induced blood brain barrier disruption. Mannitol was infused at 0.09 mL/s for 25–30 s into the carotid artery, followed immediately by 0.2 mmol/kg gadoterol (ProHance, Bracco Diagnostics) or 10 mg Fe/kg ~100-nm diameter SPIO (Ferumoxides, Berlex Laboratories). C: Localized accumulation of Gd-DTPA [top; Treat et al. (2007)] and 60-nm diameter SPIO [bottom; Liu et al. (2009)] contrast agents to rat brains following focused ultrasound (FUS) treatment, in conjunction with intravascular contrast agent delivery. Gd-DTPA (Magnevist, Berlex Laboratories) and SPIO (Resovist, Schering-Plough) doses were 125 and 15 μmol/kg, respectively. White arrows in the horizontal scans indicate sites of FUS power deposition (2 × 0.6 W top, 3 W bottom); black arrows in lower panel indicate major blood vessels. Images shown in panels (A–C) are either T_1-weighted scans (A–C, top), and T_2^*- (A, C, bottom) or T_2-weighted scans (B, bottom). Panel (A), top, reproduced with permission from Figure 1 in Mardor et al., Cancer Res, 2005, 65, 6858–6863, © American Association for Cancer Research; panel (A), bottom, reproduced with permission from the publisher, Duke University Press; panel (B), top, reproduced from Kroll et al., Neurosurgery, 1998, 43, 879–886, © Lippincott Williams & Wilkins; panel (B), bottom, reproduced from Muldoon et al., Neurosurgery, 2005, 57, 785–796, © Lippincott Williams & Wilkins; panel (C), both images, reproduced with permission from Wiley-Liss, Inc., a subsidiary of John Wiley & Sons, Inc.

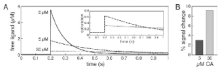

Figure 2.

Ligand buffering by responsive contrast agents. A: The dynamics of a hypothetical ligand in the brain were simulated using a single compartment kinetic model (Helmchen and Tank, 2005). In an approximation to neural signaling phenomena such as release and uptake of neurotransmitters or intracellular second messengers, a single pulse of 10 μM ligand was simulated at time 0.2 s, followed by a process that removed ligand at a rate of 20 s^{-1} on a background of weak endogenous buffering (buffer concentration 1 μM, K_d = 1 μM). The graph shows time courses of free (unbound) ligand in the presence of 0 μM (solid line), 5 μM (dashed line), or 30 μM (dotted line) of a responsive T_1 contrast agent assumed to bind the ligand with a dissociation constant of 1 μM. The simulation shows that the peak amount of free ligand, and its rate of decay back to baseline, are diminished by increasing contrast agent concentrations. The inset shows partial saturation of the contrast agent as a function of time for 5 and 30 μM concentrations. B: Peak T_1-weighted MRI signal changes were computed from the fractional saturation curves of panel (A), assuming background T_1 = 1 s, TR = 0.2 s, and ligand-induced relaxivity change from 0 to 10 mM^{-1} s^{-1}. A greater ligand-dependent signal change is observed in the presence of 30 μM contrast agent (CA), which also buffered the ligand more severely.

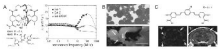

Figure 3.

MRI contrast agents for molecular and cellular imaging with improved sensitivity. A: Gd-hydroxypyridonate (Gd-HOPO)-based complexes have been designed to have characteristics optimized for high T_1 relaxivity (r_1). Key properties include the number of inner sphere water molecules (q), the exchange time for bound water (τ_M), and the rotational correlation time of the complex (τ_R). The HOPO compounds schematized at left have $q = 2$ (water ligands shown in bold) and τ_M values $\ll$ 100 ns (Cohen et al., 2000; Pierre et al., 2005); most Gd-polyaminocarboxylate complexes have less favorable $q = 1$ and τ_M 0.1–1 μs (Caravan et al., 1999). Complexes with R = CH_3 (Gd-1) or a dendrimeric substituent (Gd-2) have τ_R values of 125 and 238 ps, respectively. The longer τ_R of the larger Gd-2 complex contributes to its significantly higher r_1 across a range of magnetic field strengths, as indicated by the nuclear magnetic relaxation dispersion (NMRD) plot for Gd-2 (closed circles) and Gd-1 (open circles) shown at right. NMRD data from a more conventional macrocyclic complex, Gd-DO3A (Aime et al., 1998), is included for comparison (triangles). Theoretical curves fit to the experimental data all show a typical decline in relaxivity at high-resonance frequencies, above 100 MHz ($B_0 > 2.35$ T). B: SPIO contrast agents shown to generate particularly strong MRI effects include 1.6 μm diameter encapsulated microparticles of iron oxide (MPIOs), similar to those depicted at top. MPIOs were used to label proliferating cells in the subventricular zone (SVZ) of live rats, and visualized in sagittal gradient echo images (bottom) (Shapiro et al., 2006). The particles were infused into the ventricles near the SVZ, producing the large area of MRI signal dropout shown in the image. A narrow band of punctate T_2^* contrast is observed along the rostral migratory stream (RMS), extending from the SVZ to the olfactory bulb (white arrows). This band developed over several weeks following the injection, and is attributed to migrating cells, each harboring small numbers of MPIOs (scale bar = 5 mm). C: High sensitivity molecular neuroimaging can be achieved using MRI techniques with minimal or zero endogenous background. In this example, a fluorine-labeled analog (top, R = F) of a compound previously shown to label amyloid plaques (R = Br) (Skovronsky et al., 2000), was applied in a mouse model of Alzheimer's disease (Higuchi et al., 2005). A coronal ^{19}F MRI scan with 156 × 156 × 2000 μm resolution indicates distribution of the tracer, with no background from endogenous species (bottom left). Higher resolution anatomical data for comparison was obtained using conventional ^{1}H T_2-weighted imaging (bottom right). Arrows denote apparent amyloid deposits visible in both modalities. Several foci of ^{19}F tracer accumulation do not correspond to T_2 lesions (e.g., arrowhead, left), and may represent plaques detectable more sensitively by ^{19}F imaging. Graph in panel (A) adapted with permission from Pierre et al., J Am Chem Soc, 2005, 127, 504–505, © American Chemical Society; panel (B), top, courtesy Bangs Laboratories (Fishers, IN); panel (B), bottom, reproduced with permission from Shapiro et al., Magn Reson Med, 2006, 55, 242–249, © Wiley-Liss, Inc., a division of John Wiley & Sons, Inc.; images in panel (C) adapted with permission of the authors from Higuchi et al., Nat Neurosci, 2005, 8, 527–533, © Nature Publishing Group.